HOVERING FLIGHT FOR A MICROMECHANICAL FLYING INSECT: MODELING AND ROBUST CONTROL SYNTHESIS [1]

Luca Schenato * **Xinyan Deng** * **Shankar Sastry** *

* *Department of Electrical Engineering and Computer Sciences*
University of California at Berkeley
{*lusche|xinyan|sastry*}*@robotics.eecs.berkeley.edu*

Abstract: This paper describes recent results on the design and simulation of a flight control strategy for the Micromechanical Flying Insect (MFI), a 10-25mm (wingtip-to-wingtip) device capable of sustained autonomous flight. Biologically inspired by the real insect's flight maneuver, position control is achieved via attitude control. The wings motion is parameterized by a small set of parameters which are sufficient to generate desired average torques to regulate its attitude. Position control is achieved through attitude control based on the linearized dynamics under small angle assumption near hovering. At the end of each wingbeat, the controller schedules the desired wings motion parameters according to state feedback errors. With respect to our previous work (Deng *et al.*, 2001), we explicitly included the modeling approximations into the design of the flight controller. These errors include the time-varying nature of aerodynamic forces, the input saturation and linearization errors. The proposed controller was simulated with the Virtual Insect Flight Simulator, and the results show improved performance in both position and orientation stabilization.

Keywords: Insect Flight, Hovering, Torque Decoupling, Periodic Input, MFI

1. INTRODUCTION

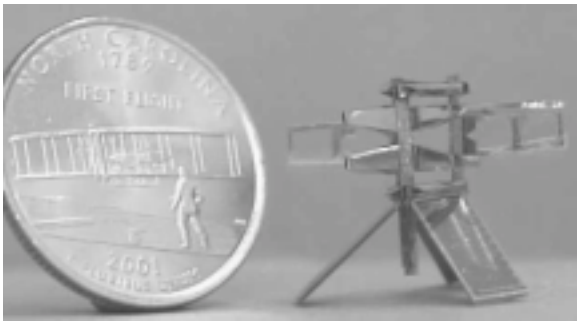

Fig. 1. MFI prototype next to a cent coin

Unmanned air vehicles (UAVs) have been a very active area of research. Despite recent remarkable achievements obtained with fixed and rotary aircrafts (Shim *et al.*, 2000), their use in many tasks is still limited by their maneuverability and size. However, the extraordinary flight capabilities of insects have inspired the design of small UAVs with flapping wings mimicking real flying insects. Their unmatched maneuverability, low fabrication cost and small size make them very attractive for cost-critical missions in environments which are unpenetrable for larger size UAVs. Moreover, the latest advances in insect flight aerodynamics and microtechnology seem to provide sufficient tools to fabricate flying insect micro-robots. This is the challenge that the Micromechanical Flying Insect project (MFI) being currently developed at UC Berkeley, has taken (Fearing *et al.*, 2000). Figure 1 shows the prototype of the robotic fly. The scope of the authors' work in this project is to model, design and eventually implement a flight control unit for the MFI. We proposed a flight control architecture (Schenato *et al.*, 2001*a*) aimed to achieve this goal, and we designed and implemented a software testbed to simulate insect flight (Schenato *et al.*, 2001*b*). In this paper we will present recent improvements in the design of the hovering controller for a MFI originally proposed in (Deng *et al.*, 2001).

[1] This work was funded by ONR MURI N00014-98-1-0671, ONR DURIP N00014-99-1-0720 and DARPA.

2. INSECT VS HELICOPTER HOVERING

Similar to aerial vehicles based on rotary wings, such as helicopter, flying insects control their flight by controlling their attitude and the magnitude of the vertical thrust (Schenato *et al.*, 2001*a*). *Position and velocity control* is achieved via attitude control: tilting and banking the body can modulate the forces acting on a plane parallel to the ground. Pitching down, for example, would result in a forward thrust, while rolling sideward would result in a lateral acceleration. *Altitude control* is achieved via mean lift modulation: increasing the vertical force would result in an upward acceleration and vice versa. However, there are some peculiar differences that prevent from applying directly the successful flight control techniques developed for helicopter (Prouty, 1995). The spinning of the rotor blade induces a reaction

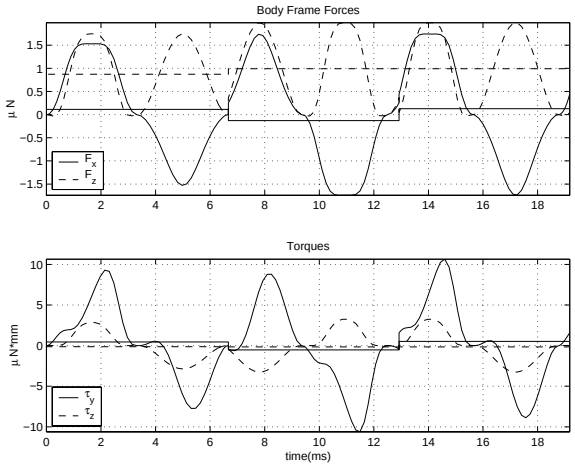

Fig. 2. Aerodynamic forces and torques in the body frame generated during three wingbeats . The piecewise constant traces correspond to the mean torque within a wingbeat.

yaw torque on the helicopter body that would make the latter rotate in the opposite sense if not compensated. This problem is not present in insect flight since the wings moves almost symmetrically on the opposite side, therefore inertial forces cancel out. Another very important difference is the intrinsic time varying nature of the aerodynamics in insect flight. As shown in Figure 2 the aerodynamic forces and torques generated by the wings are highly time varying within a wingbeat, and cannot be assumed to be constant as in case of the helicopter. Therefore, time invariant control schemes are likely to fail. One more important difference is that the wings motion can be changed at most on a wingbeat-to-wingbeat base, because the wings need to follow a periodic motion to generate sufficient lift to sustain the insect weight. Therefore, a continuous control modeling is not applicable. Finally, in insect flight the two wings can have asymmetric kinematics. This peculiar characteristic allows insect to generate large angular accelerations by modulating the distribution of the aerodynamic forces within a wingbeat, without strongly affecting the mean lift generation. Optimal wings motion for torque generation has recently been considered in (Sane and Dickinson, 2001)

These similarities and differences lead us to consider the following strategy to design a robust stabilizing hovering controller. Firstly, we will model the insect dynamics as a Discrete Time Linear Time Invariant (DTLTI) system based on the average forces and torques over a wingbeat, but we will design the controller including the approximation errors due to the time varying nature of the dynamics. Secondly, we parameterize the wing kinematics with four parameters, such that they can be mapped uniquely into the three mean torques (roll, pitch, yaw) and mean lift. This approach allows to directly control the torques and lift generation, thus simplifying the control design for the attitude and altitude of the MFI. The dynamics of the insect is then linearized about the hovering equilibrium point and we propose some approximations that decompose the original MIMO system into four SISO subsystems. Finally, the controller is based on robust state feedback based on disturbance rejection.

3. INSECT FLIGHT DYNAMICS

Recent numerical simulation of unsteady insect flight aerodynamics and experimental data based on scaled insect wings (Dickinson *et al.*, 1999), have unveiled the unsteady state aerodynamic mechanisms responsible of insect flight. From our previous work (Schenato *et al.*, 2001*b*), the aerodynamic module, that compute the lift and the drag forces of each wing based on their kinematics, is a combination of an analytical model, based on quasi-steady state assumption, and an empirically matched model based on Robofly data (**?**).

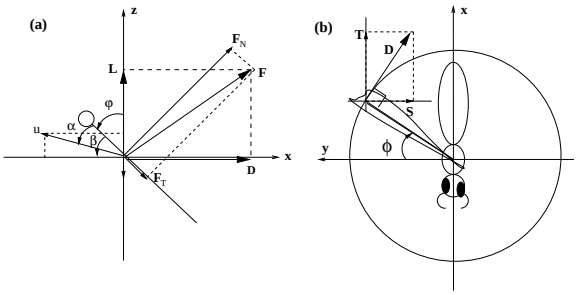

Fig. 3. Aerodynamic forces decomposed into lift(L) and drag(D) forces in stroke plane; (a) side view; (b) top view; ϕ: stroke angle, φ: rotation angle, α: angle of attack, u: wing velocity.

Given lift, drag forces and stoke angle, it is possible to derive the total wrench, i.e the forces and torques, in the *body frame*. As shown in (Murray *et al.*, 1994), the equations of motion for a rigid body subject to an external wrench $F^b = [f^b, \tau^b]^T$ applied at the center of mass and specified with respect to the body coordinate frame is given by Newton-Euler equations, which can be written as

$$\begin{aligned} \ddot{P} &= \frac{1}{m} R f^b - [0\ 0\ g]^T \\ \ddot{\Theta} &= (IW)^{-1}[\tau^b - W\dot{\Theta} \times IW\dot{\Theta} - I\dot{W}\dot{\Theta}] \end{aligned} \quad (1)$$

where the vector $P = [x\ y\ x]^T$ is the position of the center of mass, $\Theta = [\phi\ \theta\ \psi]^T$ are the Euler angles used to parameterize the rotation matrix R and the matrix W, I is the inertia matrix, and g is the gravitational acceleration.

The body forces and torques are periodic, nonlinear functions of the wing kinematics. *i.e.*

$$\begin{aligned} f^b &= f^b(\phi_i(t), \dot{\phi}_i(t), \varphi_i(t), \dot{\varphi}_i(t)) \\ \tau^b &= \tau^b(\phi_i(t), \dot{\phi}_i(t), \varphi_i(t), \dot{\varphi}_i(t)) \end{aligned} \quad (2)$$

where $i \in \{l, r\}$ represents the left and right wing, respectively.

4. AVERAGING

The dynamics of the body attitude, according to a Euler parameterization in roll pitch and yaw angles, $\Theta = [\eta\ \theta\ \psi]^T$, in the fixed frame can be written as:

$$\ddot{\Theta}(t) = u_\Theta(\Theta, \dot{\Theta}, \tau^b(t)) \quad (3)$$

where the fictitious input vector $u_\Theta \in \mathcal{R}^3$ is a nonlinear function of the body attitude, the body angular position and the torque vector $\tau^b = [\tau_\eta \ \tau_\theta \ \tau_\psi]^T$ calculated in the body frame. As already mentioned, aerodynamic forces and torques acting on the insect body are quasi-periodic and their effect on the dynamics of the insect can be difficult to describe analytically (see Figure 2).

We propose to simplify the problem by separating the mean component of the input u_Θ and from its oscillatory component. The mean torque component will be regarded as control input, while the oscillatory torque component as an external disturbance. Assuming that the three component of the control input u_Θ are independent (see Section 7), the system (3), can be rewritten in a more general state space representation as three independent SISO systems:

$$\dot{x}_i(t) = Ax_i(t) + bu_i(t) \tag{4}$$

where $x \in \mathcal{R}^2$, $u_i(\cdot) \in \mathcal{C}^0$, and the index $i \in \{\eta, \theta, \psi\}$ represent the three angles. To simplify the notation, we will drop the index i. Define the the following inputs:

$$\bar{u}_k \triangleq \int_{kT}^{(k+1)T} u(\tau)d\tau; \qquad \tilde{u}_k(t) \triangleq u(t) - \bar{u}_k \tag{5}$$

where $kT \leq t \leq (k+1)T$, and T is the period of a wingbeat. Note that $\int_{kT}^{(k+1)T} \tilde{u}_k(\tau)d\tau = 0$. Therefore we can rewrite system (4) as follows:

$$\dot{x}(t) = Ax(t) + b\bar{u}_k + b\tilde{u}_k(t) \tag{6}$$

We can now consider only the sampled state $x_k \triangleq x(kT)$ and calculate explicitly, as shown in (Callier and Dosoer, 1991), the state evolution of the discrete time system:

$$x_{k+1} = A_d x_k + b_d u_k + d_k \tag{7}$$

where the time varying component of the control input d_k appears as an external disturbance.

5. WINGS KINEMATICS PARAMETRIZATION FOR TORQUE DECOUPLING

The control scheme proposed in the previous section, implicitly assumes that we can generate the desired mean torques calculated with respect to the body frame $\tau^b = [\bar{\tau}_\eta \ \bar{\tau}_\theta \ \bar{\tau}_\psi]^T$.

Given a wings motion, described by the the stroke angles, $[\phi_r(t), \phi_l(t)]$, and rotation angles, $[\varphi_r(t), \varphi_l(t)]$, it is possible to calculate the corresponding mean torques τ^b, i.e. there is a function $g(\cdot) : (\mathcal{L}_2[0,T])^4 \to \mathcal{R}^3$ that uniquely maps the wings kinematics into the vector τ_b. The problem we need to solve is to find an inverse map $g^{-1}(\cdot)$ between the desired mean torques and kinematics for the wing pair. This task is clearly ill posed since there exist many wings kinematics that can generate the same mean torque.

An alternative approach is to parameterize the wings kinematics with only three parameters $\Pi = [\alpha_r, \alpha_l, \gamma]^T$, thus reducing the space of possible wings motions. This means that there is a function $f(\cdot) : \mathcal{R}^3 \to (\mathcal{L}_2[0,T])^4$ that maps the kinematics parameters to the wing trajectory during a wingbeat of period T. We can now define the map $\Psi(\cdot) \triangleq g \circ f(\cdot) : \mathcal{R}^3 \to \mathcal{R}^3$ between the kinematic parameters, Π, and the mean torque vector, τ^b. If the map $\Psi(\cdot)$ is, at least locally, invertible, i.e. $\Psi^{-1}(\cdot)$ exists, we can indirectly compute the desired wings kinematics through the control law $U_w \triangleq f \circ \Psi^{-1} : \mathcal{R}^3 \to (\mathcal{L}_2[0,T])^4$.

Inspired by a biomimetic approach, we first construct the function $f(\cdot)$ such that the kinematics parameters Π are strongly related with the wings biokinematics parameters that are responsible of flight in real insects. Then we find the map $\Psi(\cdot)$ via simulations, and finally compute the inverse map $\Psi^{-1}(\cdot)$, or at least its approximation. The inverse map allows to decouple the torques generation according to the following control law:

$$U_w : [\bar{\tau}_\eta, \bar{\tau}_\theta, \bar{\tau}_\psi] \to [\phi_r(t), \phi_l(t), \varphi_r(t), \varphi_l(t)]$$

The parameterization is based on recent work (Sane and Dickinson, 2001) that have evidenced how the modulation of the mean angle of attack and the phase of rotation between the two wings can generate asymmetrical instantaneous forces along a wingbeat, thus giving rise to positive or negative mean torque and forces. Intuitively, the mean angle of attack can modulate the magnitude of the aerodynamic forces on the wing: lift is maximal at an angle of attack of 45° and decreases for different angles. The advanced or delayed phase of rotation respectively increases or decreases both lift and drag at the stroke reversals.

Following these observations, we parameterize the motion of the wings with only three parameters Π as follows:

$$f : \begin{cases} \phi_r(t) = \frac{\pi}{3}\cos(2\pi ft) \\ \phi_l(t) = \frac{\pi}{3}\cos(2\pi ft) \\ \varphi_r(t) = \Upsilon_r[\sin(2\pi ft) - 0.2\alpha_r \sin^2(2\pi ft)] \\ \varphi_l(t) = \Upsilon_l[\sin(2\pi ft) - 0.2\alpha_l \sin^2(2\pi ft)] \end{cases} \tag{8}$$

$$\Upsilon_r = \frac{\pi}{4} + \frac{\pi}{8}\text{ramp}(\gamma); \quad \Upsilon_l = \frac{\pi}{4} + \frac{\pi}{8}\text{ramp}(-\gamma)$$

where $(\alpha_r, \alpha_l, \gamma) \in [-1, 1]$, $t \in [0, T]$, f is the wingbeat frequency, $T = f^{-1}$ is the wingbeat period, ψ is the stroke angle, φ is the rotation angle, and the function $\text{ramp}(\gamma) = \gamma$ if $\gamma \geq 0$ and 0 otherwise. The parameters α_r and α_l are strongly related to wing flip timing: a positive value corresponds to advancing the wing rotation on the downstroke and delaying on the upstroke, a negative value does the opposite, a null value results in a symmetric wing rotation at both the half-strokes. The parameter γ modifies the mean angle of attack of the wings: a negative value corresponds to a smaller mean angle of attack on the right wing, a positive value to the opposite, and a zero value to equal mean angle of attack.

By varying the three parameters $[\alpha_r, \alpha_l, \gamma]$, it is possible to generate sufficient torque to steer the MFI body about the roll, pitch, and yaw axes. Figure 4 and Figure 5 show the simulation results

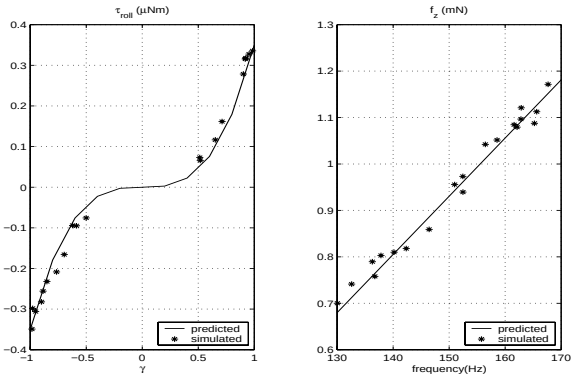

Fig. 4. Average roll torque, τ_η, map (left) as a function of the parameter γ and different values for the other two parameters (star points). The solid line corresponds to the approximate function $\tau_\eta = c\gamma^3$. Mean lift, f_z, calculated at different frequencies (right).

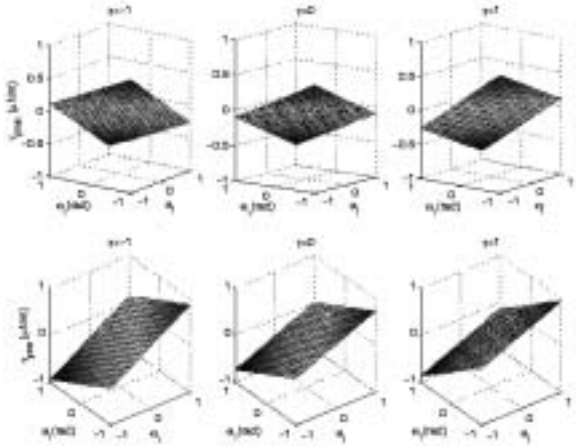

Fig. 5. Average pitch and yaw torque maps.

obtained from Virtual Insect Flight Simulator (VIFS) with the morphology of a honey bee.

We obtained an empirical map from wing kinematics to the average torque over one wingbeat $\Psi : \mathcal{R}^3_u \to \mathcal{R}^3_\tau$, via the Virtual Insect Flight Simulator (VIFS) with the morphology of a honey bee. Figure 4 and Figure 5 show the simulation results. The empirical map can be written as follows:

$$\Psi : \begin{cases} \bar{\tau}_\psi &= a_{11}\alpha_r + a_{12}\alpha_l + \delta_\psi = \hat{\tau}_\psi + \delta_\psi \\ \bar{\tau}_\theta &= a_{21}\alpha_r + a_{22}\alpha_l + \delta_\theta = \hat{\tau}_\theta + \delta_\theta \\ \bar{\tau}_\eta &= c\gamma^3 + \delta_\eta = \hat{\tau}_\eta + \delta_\eta \end{cases} \quad (9)$$

where the coefficients $a_{11}, a_{12}, a_{21}, a_{22}, c$ are constant, and $\delta_\eta, \delta_\theta, \delta_\psi$ are bounded

Consequently, given the values for the mean torques we want to generate in a wingbeat, the values for the wing parameters α_l, α_r and γ can be obtained from the inverse map, $\Psi^{-1}() : \mathcal{R}^3_\tau \to \mathcal{R}^3_u$. The function $\Psi^{-1}()$ does not necessarily exist or can be hard to find in practice. It depends on the chosen parameterization of the wings motion and on the velocity of the insect body. For the wing parameterization (8) the inverse map $\Psi^{-1}()$ is approximated as follows:

$$\hat{\Psi}^{-1} : \begin{cases} \hat{\gamma} &= \text{sat}\big[c^{-\frac{1}{3}}\,\hat{\tau}_\eta^{\frac{1}{3}}\big] \\ \hat{\alpha}_l &= \text{sat}\big[b_{11}\,\hat{\tau}_\theta + b_{12}\,\hat{\tau}_\psi\big] \\ \hat{\alpha}_r &= \text{sat}\big[b_{21}\,\hat{\tau}_\theta + b_{22}\,\hat{\tau}_\psi\big] \end{cases} \quad (10)$$

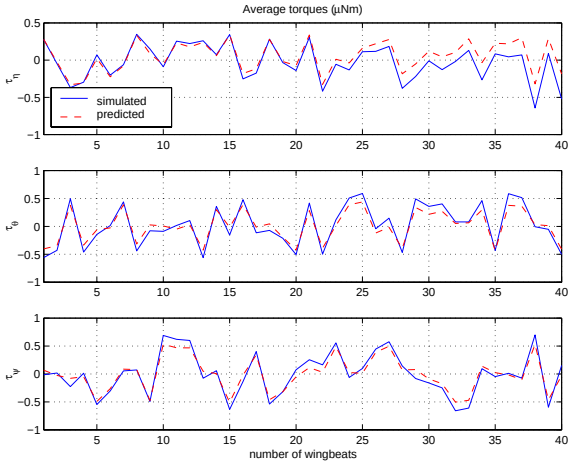

Fig. 6. Comparison of the average torques calculated from approximate functions and those from the simulation, over a consecutive 40 wingbeats; γ, α_l,and α_r are chosen randomly.

where the parameters, $c, b_{11}, b_{12}, b_{21}, b_{22}$ are constant, and the saturation function $\text{sat}(u) = u$ for $|u| \leq 1$ and $\text{sat}(u) = \frac{u}{|u|}$ otherwise.

The saturation function takes into account kinematics limitations of the wings. As we expected, the parameter γ influences the roll torque, but is almost decoupled from the yaw and pitch torques. The parameters α_r, α_l are coupled together, but quite surprisingly, in a linear fashion, which is very helpful from an implementation prospective. In order to evaluate the approximation map in a more realistic setting, we simulate the MFI motion in VIFS by randomly choosing the value of the parameters $(\gamma, \alpha_l, \alpha_r)$ for a consecutively 40 wingbeats. In this setting, coupling factors among the parameters and insect body velocities are taken into account. Figure 6 shows the mean yaw torque predicted by the approximate map $\hat{\Psi}^{-1}()$ and the mean torque per wingbeat actually calculated from the simulation, corresponding to the real map $f()$. It shows that the approximate map matches the real value very well and is very promising in the prospective of designing feedback control.

6. LINEARIZED HOVERING DYNAMICS

Hovering flight mode is characterized by small body velocity and angular deviations. Therefore, we will linearize the insect dynamics insect described by Equations (1), about the hovering state $[P, \Theta, \dot{P}, \dot{\Theta}] = [0, 0, 0, 0]$:

The aerodynamic force vector, $f^b(t)$, and the torque vector, $\tau^b(t)$, are quasi-periodic signals. Following the argument argument presented in Section 4, we arbitrarily decompose the signals into their means and their zero-mean oscillatory component within every wingbeat. Simulations obtained with VIFS (see Figures 2) show that the force and torque vectors can be written as:

$$f^b(t) = \begin{bmatrix} 0 \\ 0 \\ af^2 \end{bmatrix} + \begin{bmatrix} d_x(t) \\ d_y(t) \\ d_z(t) \end{bmatrix}; \quad \tau^b(t) = \begin{bmatrix} \bar{\tau}_\eta \\ \bar{\tau}_\theta \\ \bar{\tau}_\psi \end{bmatrix} + \begin{bmatrix} d_\eta(t) \\ d_\theta(t) \\ d_\psi(t) \end{bmatrix} \quad (11)$$

where a is a constant, f is the wingbeat frequency, and the vectors $d_P = [d_x, d_y, d_z]$ and $d_\Theta = [d_\eta, d_\theta, d_\psi]$ are zero-mean signals. The mean vector force corresponds, not surprisingly, to the mean lift generated by the insect.

Substituting the Equations (11) into (1), we get:

$$\begin{aligned}
\ddot{x} &= m^{-1}[af^2\,\theta - \psi\,d_y(t) + \theta\,d_z(t)] + o(||\Theta||^2)\\
\ddot{y} &= m^{-1}[-af^2\,\eta + \psi\,d_x(t) - \eta\,d_z(t)] + o(||\Theta||^2)\\
\ddot{z} &= m^{-1}[af^2 - \theta\,d_x(t) + \eta\,d_y(t)] - g + o(||\Theta||^2)\\
\ddot{\eta} &= I_\eta^{-1}[\bar{\tau}_\eta + d_\eta(t) - \theta\,d_\psi(t)] + o(||\Theta||^2) + o(||\dot{\Theta}||^2)\\
\ddot{\theta} &= I_\theta^{-1}[\bar{\tau}_\theta + d_\theta(t) + \eta\,d_\psi(t)] + o(||\Theta||^2) + o(||\dot{\Theta}||^2)\\
\ddot{\psi} &= I_\psi^{-1}[\bar{\tau}_\psi + d_\psi(t) - \eta\,d_\theta(t)] + o(||\Theta||^2) + o(||\dot{\Theta}||^2)
\end{aligned}$$

where the rotation matrix R and the matrix W have been linearized about the hovering orientation $\Theta = 0$ (Murray *et al.*, 1994). We want to linearize this system about the hovering condition $[P, \dot{P}, \Theta, \dot{\Theta}] = [0, 0, 0, 0]$. This requires that $m^{-1}af^2 - g = 0$. We define the hovering frequency $f_0 \triangleq \sqrt{\frac{mg}{a}}$, and we linearize the dynamics of the insects about f_0, such that:

$$m^{-1}af^2 = g + \frac{g}{f_0}(f - f_0) + o(||f - f_0||^2) \quad (12)$$

We define the control input vector $u = [u_\eta\ u_\theta\ u_\psi\ u_z]^T$ as follows :

$$\Xi : \begin{cases} f &= f_0\,(1 + \rho \mathrm{sat}(u_z)) \\ \hat{\tau}_\psi &= u_\psi \\ \hat{\tau}_\theta &= u_\theta \\ \hat{\tau}_\eta &= u_\eta \end{cases} \quad (13)$$

where the range of the wingbeat frequency f is saturated to take into account kinematic limitation of the wings. The factor ρ relates to the maximum variation of the frequency.

By close inspection of these equations, it is evident that there is only a weak coupling between the dynamics among some variables. Moreover, the limited frequency control input, $|u_z| \leq 1$ has only limited effect on the dynamics of x and y. This weak coupling can be modeled as external disturbances. Since we are considering hovering control, we assume that the attitude angles are limited, i.e. $||\Theta||_\infty \leq \varepsilon$.

Substituting Equations (13) and (10) into Equations (12) we obtain the linearized dynamics of the system S:

$$\begin{cases} \ddot{x} &= g(1 + \rho\,\delta_z)\theta + m^{-1}d_z(t) - \varepsilon m^{-1}d_y(t) \\ \ddot{y} &= -g(1 + \rho\,\delta_z)\eta - m^{-1}d_z(t) + \varepsilon m^{-1}d_x(t) \\ \ddot{z} &= \rho g\,u_z - \varepsilon m^{-1}d_x(t) + \varepsilon m^{-1}d_y(t) \\ \ddot{\eta} &= I_\eta^{-1}\,u_\eta + I_\eta^{-1}\,\delta_\eta + I_\eta^{-1}d_\eta(t) - \varepsilon I_\eta^{-1}d_\psi(t) \\ \ddot{\theta} &= I_\theta^{-1}\,u_\theta + I_\theta^{-1}\,\delta_\theta + I_\theta^{-1}d_\theta(t) + \varepsilon I_\theta^{-1}d_\psi(t) \\ \ddot{\psi} &= I_\psi^{-1}\,u_\psi + I_\psi^{-1}\,\delta_\psi + I_\psi^{-1}d_\psi(t) - \varepsilon I_\psi^{-1}d_\theta(t) \end{cases} \quad (14)$$

where the disturbance $\delta_z \in [-1, 1]$ is unknown.

This simplified dynamics greatly reduces the complexity of the controller. In fact, from Equations (12) and (12), it is evident that there is coupling only between the dynamics of x and the pitch θ, and between the dynamics of y and the roll η. The weak coupling with the other states has been modeled as an external disturbance. If the flight controller is guaranteed to stabilize the simplified system S, then it will also stabilize the original system (1). The system S can be written in state space representation as follows:

$$\begin{aligned}
S_1 :&\ \dot{x}_1 = (A_1 + \Delta_1)\,x_1 + b_1\,u_\theta + E_1\,d(t)\\
S_2 :&\ \dot{x}_2 = (A_2 + \Delta_2)\,x_2 + b_2\,u_\eta + E_2\,d(t)\\
S_3 :&\ \dot{x}_3 = A_3\,x_3 + b_3\,u_\psi + E_3\,d(t)\\
S_4 :&\ \dot{x}_4 = A_4\,x_4 + b_4\,u_z + E_4\,d(t)
\end{aligned}$$

where $x_1 = [x, \theta, \dot{x}, \dot{\theta}]$, $x_2 = [y, \eta, \dot{y}, \dot{\eta}]$, $x_3 = [\psi, \dot{\psi}]$, $x_4 = [z, \dot{z}]$, and $d = [d_x, d_y, d_z, d_\eta, d_\theta, d_\psi]$. The explicit description of matrices $\{A_i, b_i, e_i\}$ is not given here because of space limitation.

7. CONTROL DESIGN

As described in Section 4, we assume we can control the mean of the control inputs within a wingbeat. Therefore we will design the controllers based on the discretized system S^d:

$$\begin{aligned}
S_1^d :&\ x_1^{k+1} = (A_1^d + \Delta_1^d)\,x_1^k + b_1^d\,u_\theta^k + E_1^d\,d^k\\
S_2^d :&\ x_2^{k+1} = (A_2^d + \Delta_2^d)\,x_2^k + b_2^d\,u_\eta^k + E_2^d\,d^k\\
S_3^d :&\ x_3^{k+1} = A_3^d\,x_3^k + b_3^d\,u_\psi^k + E_3^d\,d^k\\
S_4^d :&\ x_4^{k+1} = A_4^d\,x_4^k + b_4^d\,u_z^k + E_4^d\,d^k
\end{aligned}$$

where $x^k = x(kT)$, and the matrices for the discrete time system S^d have been derived from the continuous time system S as explained in Section 4.

The overall dynamics can be modeled with 4 decoupled DTLTI SISO systems with external disturbances, dynamic uncertainty, and input saturation. There are several approaches to design stabilizing feedback control law: PID, variable structure control (VSC), robust control. We decided to implement a simple state feedback based on pole placement:

$$u : \begin{cases} u_\theta^k &= -k_0^\theta x^k - k_1^\theta \dot{x}^k - k_2^\theta \theta^k - k_3^\theta \dot{\theta}^k \\ u_\eta^k &= -k_0^\eta y^k - k_1^\eta \dot{y}^k - k_2^\eta \eta^k - k_3^\eta \dot{\eta}^k \\ u_\psi^k &= -k_0^\psi \psi^k - k_1^\psi \dot{\psi}^k \\ u_z^k &= -k_0^z z^k - k_1^z \dot{z}^k \end{cases} \quad (15)$$

The poles are placed taking into account input saturation, external disturbances and the uncertain dynamics approximation. The overall control scheme is obtained by cascading Equations (15), (13), (10) and (8).

The proposed control method is simulated with VIFS (Schenato *et al.*, 2001*b*) for a continuous 200 wingbeats. Figure 7 shows the resulting position and velocity trajectories, together with the corresponding parameters chosen at each wingbeat. The linear and angular displacements are recovered from $[15\ \ 40\ \ -20]$ millimeters and $[30^o\ \ -45^o\ \ \ 60^o]$ to its equilibrium point within 600

milliseconds in less than 90 wingbeats. It shows that the controller succeeds in stabilizing hovering and control both position and attitude. The MFI shows a small chattering motion about the equilibrium position. This unavoidable phenomenon is mainly due to the periodic motion of the flapping wing, and also due to the fact that nonlinearity and coupling among dynamic variables have been neglected.

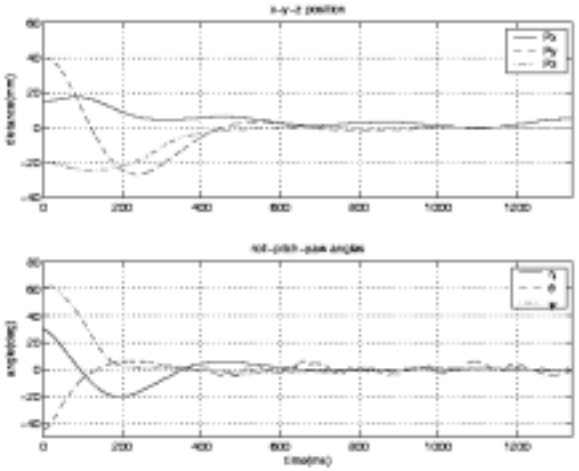

Fig. 7. MFI position and orientation trajectories.

8. SIMULATION RESULTS

The proposed control method is simulated with VIFS (Schenato *et al.*, 2001*b*) for a continuous 200 wingbeats and Figure 7 shows the resulting position and orientation trajectories. The linear and angular displacements are recovered from $[15\ 40\ -20]$ millimeters and $[30^o\ -45^o\ 60^o]$ to its equilibrium point within 600 milliseconds in less than 90 wingbeats. It shows that the controller succeeds in stabilizing hovering and controls both position and attitude. Moreover, the MFI shows a chattering motion about the equilibrium position. This phenomenon is mainly due to the periodic motion of the flapping wing, and also due to the fact that nonlinearity and coupling among dynamic variables have been neglected.

9. CONCLUSIONS

In this work, we have parameterized the wing kinematics by a small set of parameters to decouple the control of the average torques generated by the wings. Based on the inverse map of the parameter and mean torques, a controller was designed to schedule the desired wings motion based on the feedback error at the end of each wingbeat. The model of the linearized dynamics under the small angle assumption, takes into account of the most important modeling errors and disturbances that were neglected in our previous work (Deng *et al.*, 2001). This new controller design succeeds in robustly regulating MFI's attitude and position. Moreover, it reduces the ad hoc tuning of the gains, since parameter are optimized including MFI realistic limitations.

In order to simplify the model, we did not take into account external disturbances such as wind gusts and rain. However, our goal is to design a controller with a large basin of stability, such that the MFI is able to recover the hovering flight mode even from an upside-down position. As a consequence, albeit wind gusts and rain may degrade flight performance, they should not compromise the overall behavior of the MFI. We will address this issue in future work. Another major assumption was the full access to the insect states. In practice, perfect state information is not available. However, the MFI will be equipped with various sensors such as halteres (Wu *et al.*, 2002), flow sensors and light detectors, which are currently under investigation. Therefore, future work will also address sensor modeling and output feedback.

10. REFERENCES

Callier, F.M. and C.A. Dosoer (1991). *Linear System Theory*. Springer Verlag.

Deng, X., L. Schenato and S.S. Sastry (2001). Hovering flight control of a micromechanical flying insect. In: *Proc. of the IEEE Conf. on Decision and Control*. Orlando, USA.

Dickinson, M.H., F.O. Lehnmann and S.S. Sane (1999). Wing rotation and the aerodynamic basis of insect flight. *Science* **284**(5422), 1954–1960.

Fearing, R.S., K.H. Chiang, M.H. Dickinson, D.L. Pick, M. Sitti and J. Yan (2000). Transmission mechanism for a micromechanical flying insect. In: *Proc. of the IEEE Int. Conf. on Robotics and Automation*. pp. 1509–1515.

Murray, R. M., Z. Li and S.S. Sastry (1994). *A Mathematical Introduction to Robotic Manipulation*. CRC Press.

Prouty, R.W. (1995). *Helicopter Performance, Stability and Control*. Krieger Publishing Company.

Sane, S. P. and M. H. Dickinson (2001). The control of flight force by a flapping wing: Lift and drag production. *Experimental Biology* **204**(204), 2607–2626.

Schenato, L., X. Deng and S.S. Sastry (2001*a*). Flight control system for a micromechanical flying insect. In: *Proc. of the IEEE Int. Conf. on Robotics and Automation*. Seoul, Korea.

Schenato, L., X. Deng, W.C. Wu and S.S. Sastry (2001*b*). Virtual insect flight simulator (VIFS): A software testbed for insect flight. In: *Proc. of the IEEE Int. Conf. on Robotics and Automation*. Seoul, Korea.

Shim, D. H., H. J. Kim and S.S. Sastry (2000). Control system design for rotorcraft-based unmanned aerial vehicles using time-domain system identification. In: *Proc. of the IEEE Int. Conf. on Control Applications*. Anchorage, USA.

Wu, W.C., R.J. Wood and R.S. Fearing (2002). The halteres for the micromechanical flying insect. In: *Proc. of the IEEE Int. Conf. on Robotics and Automation*. Washington DC.